

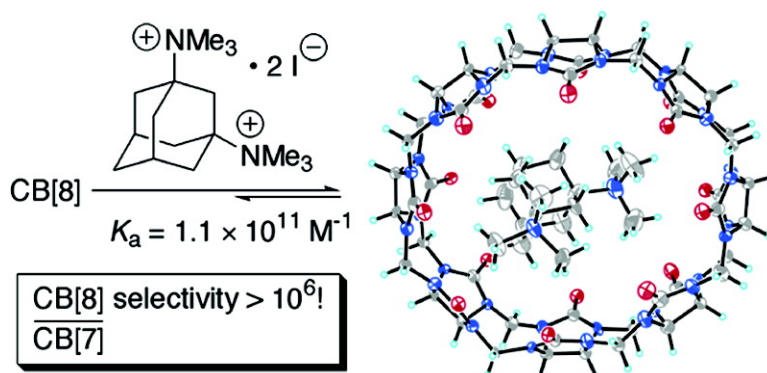
Article

**The Cucurbit[*n*]uril Family: Prime Components for Self-Sorting Systems**

Simin Liu, Christian Ruspic, Pritam Mukhopadhyay, Sriparna Chakrabarti, Peter Y. Zavalij, and Lyle Isaacs

*J. Am. Chem. Soc.*, **2005**, 127 (45), 15959-15967 • DOI: 10.1021/ja055013x • Publication Date (Web): 21 October 2005

Downloaded from <http://pubs.acs.org> on March 25, 2009



**More About This Article**

Additional resources and features associated with this article are available within the HTML version:

- Supporting Information
- Links to the 48 articles that cite this article, as of the time of this article download
- Access to high resolution figures
- Links to articles and content related to this article
- Copyright permission to reproduce figures and/or text from this article

[View the Full Text HTML](#)

## The Cucurbit[*n*]uril Family: Prime Components for Self-Sorting Systems

Simin Liu, Christian Ruspic,<sup>†</sup> Pritam Mukhopadhyay, Sriparna Chakrabarti, Peter Y. Zavalij, and Lyle Isaacs\*

Contribution from the Department of Chemistry and Biochemistry, University of Maryland, College Park, Maryland 20742

Received July 25, 2005; E-mail: LIsaacs@umd.edu

**Abstract:** We determined the values of  $K_a$  for a wide range of host–guest complexes of cucurbit[*n*]uril (CB[*n*]), where  $n = 6–8$ , using <sup>1</sup>H NMR competition experiments referenced to absolute binding constants measured by UV/vis titration. We find that the larger homologues—CB[7] and CB[8]—individually maintain the size, shape, and functional group selectivity that typifies the recognition behavior of CB[6]. The cavity of CB[7] is found to effectively host trimethylsilyl groups. Remarkably, the values of  $K_a$  for the interaction of CB[7] with adamantane derivatives **22–24** exceeds  $10^{12} \text{ M}^{-1}$ . The high levels of selectivity observed for each CB[*n*] *individually* is also observed for the CB[*n*] family *collectively*. That is, the selectivities of CB[6], CB[7], and CB[8] toward a common guest can be remarkably large. For example, guests **1**, **3**, and **11** prefer CB[8] relative to CB[7] by factors greater than  $10^7$ ,  $10^6$ , and 3000, respectively. Conversely, guests **23** and **24** prefer CB[7] relative to CB[8] by factors greater than 5100 and 990, respectively. The high levels of selectivity observed *individually and collectively* for the CB[*n*] family renders them prime components for the preparation of functional biomimetic self-sorting systems.

### Introduction

One of the grand challenges for chemistry and biology is the delineation of the design principles that endow large collections of molecules with the ability to exhibit life processes (e.g. controlled motion, reproduction, sensing, and self-defense). An examination of the behavior of the most common biomolecules (e.g. proteins, nucleic acids, oligosaccharides, antibodies) suggests that a key component in the generation of life-like complexity and function is the availability of compounds that recognize and transform other components within a complex mixture in recognition events of high affinity and fidelity. As a first step toward mimicking some of the complexity of natural systems, we have begun to create complex mixtures of synthetic compounds with the long-term goal of reproducing some of these remarkable behaviors. We have recently demonstrated that the preparation of self-sorting systems in CDCl<sub>3</sub> and H<sub>2</sub>O—collections of components that efficiently distinguish between self and nonself to generate a single set of aggregates at thermodynamic equilibrium—is as straightforward as selecting the components of a series of well-defined aggregates from the literature provided they possess different presentations of their H-bonding groups (e.g. H-bond number, pattern, and geometrical distribution) or distinct interaction interfaces (e.g. size, shape, and electrostatic complementarity).<sup>1–3</sup> The number of synthetic

host families, however, that display biomolecule range affinity ( $K_d < 1 \mu\text{M}$ ;  $K_a > 10^6 \text{ M}^{-1}$ ), selectivity, or catalytic activity, particularly for studies in aqueous solution, is limited to certain cyclophanes,<sup>4</sup> self-assembled receptors,<sup>5</sup> and the cucurbit[*n*]uril (CB[*n*]) family.<sup>6–8</sup> In this paper, we argue that the CB[*n*] family of macrocycles possesses a confluence of properties that makes them ideal components for complex self-sorting systems.

The CB[*n*] family comprises a series of macrocyclic methylene-bridged glycoluril oligomers containing *n* glycoluril units<sup>9,10</sup> as well as CB[*n*] derivatives,<sup>11</sup> analogues,<sup>12</sup> and

- (4) *Molecular Recognition: Receptors for Molecular Guests*; Vögtle, F., Ed.; Pergamon: Oxford, 1996; Vol. 2.
- (5) Rebeck, J., Jr. *Angew. Chem., Int. Ed.* **2005**, *44*, 2068–2078. Yoshizawa, M.; Nakagawa, J.; Kumazawa, K.; Nagao, M.; Kawano, M.; Ozeki, T.; Fujita, M. *Angew. Chem., Int. Ed.* **2005**, *44*, 2151–2154. Gibb, C. L. D.; Gibb, B. C. *J. Am. Chem. Soc.* **2004**, *126*, 11408–11409. Davis, A. V.; Raymond, K. N. *J. Am. Chem. Soc.* **2005**, *127*, 7912–7919.
- (6) Lagona, J.; Mukhopadhyay, P.; Chakrabarti, S.; Isaacs, L. *Angew. Chem., Int. Ed.* **2005**, *44*, 4844–4870.
- (7) Lee, J. W.; Samal, S.; Selvapalam, N.; Kim, H.-J.; Kim, K. *Acc. Chem. Res.* **2003**, *36*, 621–630.
- (8) Mock, W. L. *Top. Curr. Chem.* **1995**, *175*, 1–24.
- (9) Kim, J.; Jung, I.-S.; Kim, S.-Y.; Lee, E.; Kang, J.-K.; Sakamoto, S.; Yamaguchi, K.; Kim, K. *J. Am. Chem. Soc.* **2000**, *122*, 540–541. Day, A. I.; Blanch, R. J.; Arnold, A. P.; Lorenzo, S.; Lewis, G. R.; Dance, I. *Angew. Chem., Int. Ed.* **2002**, *41*, 275–277.
- (10) Day, A. I.; Arnold, A. P.; Blanch, R. J.; Snushall, B. *J. Org. Chem.* **2001**, *66*, 8094–8100.
- (11) Flinn, A.; Hough, G. C.; Stoddart, J. F.; Williams, D. J. *Angew. Chem., Int. Ed. Engl.* **1992**, *31*, 1475–1477. Zhao, J.; Kim, H.-J.; Oh, J.; Kim, S.-Y.; Lee, J. W.; Sakamoto, S.; Yamaguchi, K.; Kim, K. *Angew. Chem., Int. Ed.* **2001**, *40*, 4233–4235. Isobe, H.; Sato, S.; Nakamura, E. *Org. Lett.* **2002**, *4*, 1287–1289; Day, A. I.; Arnold, A. P.; Blanch, R. J. *Molecules* **2003**, *8*, 74–84. Jon, S. Y.; Selvapalam, N.; Oh, D. H.; Kang, J.-K.; Kim, S.-Y.; Jeon, Y. J.; Lee, J. W.; Kim, K. *J. Am. Chem. Soc.* **2003**, *125*, 10186–10187. Zhao, Y.; Xue, S.; Zhu, Q.; Tao, Z.; Zhang, J.; Wei, Z.; Long, L.; Hu, M.; Xiao, H.; Day, A. I. *Chin. Sci. Bull.* **2004**, *49*, 1111–1116. Lee, H.-K.; Park, K. M.; Jeon, Y. J.; Kim, D.; Oh, D. H.; Kim, H. S.; Park, C. K.; Kim, K. *J. Am. Chem. Soc.* **2005**, *127*, 5006–5007.

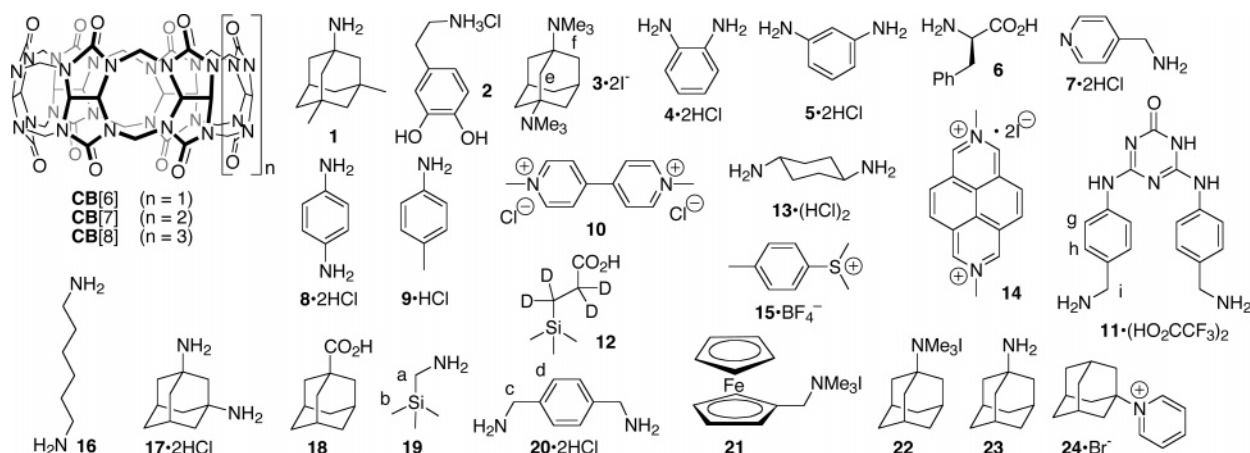
<sup>†</sup> C.R. was an undergraduate exchange student from the Institut für Organische Chemie, Universität Duisburg-Essen, 45117 Essen, Germany.

(1) Wu, A.; Isaacs, L. *J. Am. Chem. Soc.* **2003**, *125*, 4831–4835.

(2) Mukhopadhyay, P.; Wu, A.; Isaacs, L. *J. Org. Chem.* **2004**, *69*, 6157–6164.

(3) Wu, A.; Chakraborty, A.; Fettingner, J. C.; Flowers, R. A., II; Isaacs, L. *Angew. Chem., Int. Ed.* **2002**, *41*, 4028–4031.

Chart 1. Guests Used in This Paper



congeners.<sup>13</sup> The molecular recognition and self-assembly properties of CB[6]<sup>14</sup>—the oldest and most widely studied member of the CB[*n*] family—have been delineated by the pioneering work of Mock<sup>15,16</sup> and Kim.<sup>17,18</sup> CB[6] undergoes high affinity, highly selective, constrictive binding interactions with cationic species, especially ammonium ions, driven by a combination of ion–dipole interactions, hydrogen bonds, and the hydrophobic effect. Aside from well-defined thermodynamic effects, CB[6] also excels from the viewpoint of kinetic control of recognition processes.<sup>19</sup> For example, CB[6] accelerates the dipolar cycloaddition between acetylenes and azides.<sup>20</sup> Furthermore, Nau has recently demonstrated that the kinetics of binding can be tuned by guest structure and experimental conditions (e.g., pH, cation identity, and cation concentration).<sup>21</sup> This set of properties makes CB[6] an attractive component in nanotechnology, including molecular machines, supramolecular self-assembly, and crystal engineering. In recent work, several groups have begun to investigate the recognition and catalytic properties of CB[7]<sup>22–26</sup> and CB[8]<sup>27–30</sup> and chemical or physical methods

to control those processes, which suggests that CB[7] and CB[8], *independently*, will prove as useful as CB[6] for nanotechnology applications.<sup>6,7</sup> In this paper, we argue that the CB[*n*] family, *collectively*, constitute prime components for the preparation of complex self-sorting systems not only because of the well-defined recognition properties (e.g. affinity and selectivity) of each member of the family but also because of the high levels of selectivity exhibited by *different members of the family for a common guest*.<sup>31</sup>

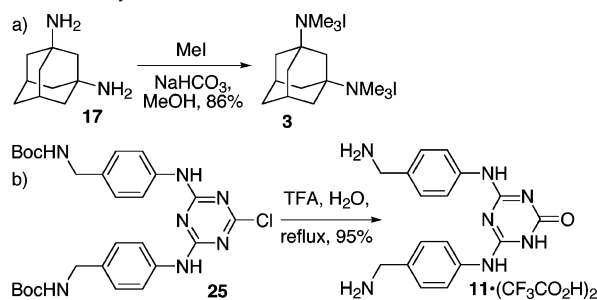
## Results

Several groups have determined the binding constants of CB[7] and CB[8] toward different guest molecules,<sup>23–26,29,30,32,33</sup> and some have reported qualitative investigations of the binding of CB[5]–CB[8] toward a common guest (e.g. guest inclusion or exclusion).<sup>34</sup> In this paper, we report the binding constants of CB[6], CB[7], and CB[8] toward a variety of guests that demonstrates that the high selectivity seen by single members of the CB[*n*] family also translates *between* members of the CB[*n*] family. For this purpose, we have employed <sup>1</sup>H NMR competition experiments<sup>15</sup> referenced to an absolute *K<sub>a</sub>* value determined by UV/vis titration.

**Selection of Guests.** Chart 1 shows the chemical structures of the guests (1–24) studied in this paper. Our selection of these guests is based on literature precedent and our own experience with the binding properties of the CB[*n*] family.<sup>2,12,13</sup> Ideally, guests should experience changes in their UV/vis or fluorescence spectra upon binding, exhibit slow exchange kinetics between free and bound guest on the <sup>1</sup>H NMR chemical shift time scale,

- (12) Lagona, J.; Fettingner, J. C.; Isaacs, L. *Org. Lett.* **2003**, *5*, 3745–3747.  
 (13) Burnett, C. A.; Witt, D.; Fettingner, J. C.; Isaacs, L. *J. Org. Chem.* **2003**, *68*, 6184–6191.  
 (14) Freeman, W. A.; Mock, W. L.; Shih, N. Y. *J. Am. Chem. Soc.* **1981**, *103*, 7367–7368.  
 (15) Mock, W. L.; Shih, N. Y. *J. Org. Chem.* **1986**, *51*, 4440–4446.  
 (16) Mock, W. L.; Shih, N. Y. *J. Am. Chem. Soc.* **1988**, *110*, 4706–4710.  
 (17) Jeon, Y.-M.; Kim, J.; Whang, D.; Kim, K. *J. Am. Chem. Soc.* **1996**, *118*, 9790–9791.  
 (18) Whang, D.; Park, K.-M.; Heo, J.; Ashton, P.; Kim, K. *J. Am. Chem. Soc.* **1998**, *120*, 4899–4900. Isobe, H.; Tomita, N.; Lee, J. W.; Kim, H.-J.; Kim, K.; Nakamura, E. *Angew. Chem., Int. Ed.* **2000**, *39*, 4257–4260. Lee, E.; Heo, J.; Kim, K. *Angew. Chem., Int. Ed.* **2000**, *39*, 2699–2701.  
 (19) Mock, W. L.; Shih, N. Y. *J. Am. Chem. Soc.* **1989**, *111*, 2697–2699.  
 (20) Mock, W. L.; Irra, T. A.; Wepsiec, J. P.; Adhya, M. *J. Org. Chem.* **1989**, *54*, 5302–5308; Tuncel, D.; Steinke, J. H. G. *Macromolecules* **2004**, *37*, 288–302.  
 (21) Marquez, C.; Hudgins, R. R.; Nau, W. M. *J. Am. Chem. Soc.* **2004**, *126*, 5808–5816; Marquez, C.; Nau, W. M. *Angew. Chem., Int. Ed.* **2001**, *40*, 3155–3160.  
 (22) Ong, W.; Kaifer, A. E. *Angew. Chem., Int. Ed.* **2003**, *42*, 2164–2167; Sindelar, V.; Moon, K.; Kaifer, A. E. *Org. Lett.* **2004**, *6*, 2665–2668; Marquez, C.; Nau, W. M. *Angew. Chem., Int. Ed.* **2001**, *40*, 4387–4390; Marquez, C.; Pischel, U.; Nau, W. M. *Org. Lett.* **2003**, *5*, 3911–3914; Mohanty, J.; Nau, W. M. *Angew. Chem., Int. Ed.* **2005**, *44*, 3750–3754; Lorenzo, S.; Day, A.; Craig, D.; Blanch, R.; Arnold, A.; Dance, I. *CrystEngComm* **2001**, *1*, 49; Blanch, R. J.; Sleeman, A. J.; White, T. J.; Arnold, A. P.; Day, A. I. *Nano Lett.* **2002**, *2*, 147–149; Shen, Y.; Xue, S.; Zhao, Y.; Zhu, Q.; Tao, Z. *Chin. Sci. Bull.* **2003**, *48*, 2694–2697; Xu, L.; Liu, S.-M.; Wu, C.-T.; Feng, Y.-Q. *Electrophoresis* **2004**, *25*, 3300–3306.  
 (23) Ong, W.; Kaifer, A. E. *J. Org. Chem.* **2004**, *69*, 1383–1385.  
 (24) Sindelar, V.; Cejas, M. A.; Raymo, F. M.; Kaifer, A. E. *New J. Chem.* **2005**, *29*, 280–282.  
 (25) Choi, S.; Park, S. H.; Ziganshina, A. Y.; Ko, Y. H.; Lee, J. W.; Kim, K. *Chem. Commun.* **2003**, 2176–2177.  
 (26) Kim, H.-J.; Jeon, W. S.; Ko, Y. H.; Kim, K. *Proc. Natl. Acad. Sci. U.S.A.* **2002**, *99*, 5007–5011.

- (27) Jon, S. Y.; Ko, Y. H.; Park, S. H.; Kim, H.-J.; Kim, K. *Chem. Commun.* **2001**, 1938–1939; Pattabiraman, M.; Natarajan, A.; Kaanumalle, L. S.; Ramamurthy, V. *Org. Lett.* **2005**, *7*, 529–532; Moon, K.; Grindstaff, J.; Sobransingh, D.; Kaifer, A. E. *Angew. Chem., Int. Ed.* **2004**, *43*, 5496–5499.  
 (28) Kim, S.-Y.; Jung, I.-S.; Lee, E.; Kim, J.; Sakamoto, S.; Yamaguchi, K.; Kim, K. *Angew. Chem., Int. Ed.* **2001**, *40*, 2119–2121. Kim, K.; Kim, D.; Lee, J. W.; Ko, Y. H.; Kim, K. *Chem. Commun.* **2004**, *2004*, 848–849. Ko, Y. H.; Kim, K.; Kang, J.-K.; Chun, H.; Lee, J. W.; Sakamoto, S.; Yamaguchi, K.; Fettingner, J. C.; Kim, K. *J. Am. Chem. Soc.* **2004**, *126*, 1932–1933. Lee, J. W.; Kim, K.; Choi, S.; Ko, Y. H.; Sakamoto, S.; Yamaguchi, K.; Kim, K. *Chem. Commun.* **2002**, 2692–2693. Liu, J.-X.; Tao, Z.; Xue, S.-F.; Zhu, Q.-J.; Zhang, J.-X. *Wuji Huaxue Xuebao* **2004**, *20*, 139–146. Fu, H.; Xue, S.; Mu, L.; Du, Y.; Zhu, Q.; Tao, Z.; Zhang, J.; Day, A. I. *Sci. China Ser. B* **2004**, *34*, 517–525. Chubarova, E. V.; Samsonenko, D. G.; Sokolov, M. N.; Gerasko, O. A.; Fedin, V. P.; Platas, J. G. *J. Inclusion Phenom. Macrocycl. Chem.* **2004**, *48*, 31–35.  
 (29) Kim, H.-J.; Heo, J.; Jeon, W. S.; Lee, E.; Kim, J.; Sakamoto, S.; Yamaguchi, K.; Kim, K. *Angew. Chem., Int. Ed.* **2001**, *40*, 1526–1529.  
 (30) Ziganshina, A. Y.; Ko, Y. H.; Jeon, W. S.; Kim, K. *Chem. Commun.* **2004**, 806–807.

Scheme 1. Synthesis of **3** and **11**

and display a range of binding free energies. For example, aliphatic and aromatic amines are well-known to bind to CB[6], whereas the more spacious cavities of CB[7] and CB[8] have been reported to host larger guests such as viologen, ferrocene, and adamantane derivatives.<sup>7,23–26,29,30,32,33</sup>

**Synthesis of Compounds **3** and **11**.** The majority of the compounds used in this study were commercially available. CB[6]–CB[8],<sup>10</sup> **17**,<sup>35</sup> and **25**<sup>36</sup> were prepared according to literature procedures. Scheme 1 shows the synthesis of new compounds **3** and **11**. Compound **3** was prepared by the alkylation of **17** with MeI in 86% yield. Melamine-derived guest **11** was prepared by the deprotection reaction of **25** with aqueous TFA; this compound is depicted as its N–H tautomer based on the X-ray crystal structure of its CB[8] complex (*vide infra*).

**Selection of a Common Buffer.** A key consideration in planning our studies was the choice of a buffer system. For example, whereas CB[7] is quite soluble in H<sub>2</sub>O, CB[6] and CB[8] have poor solubility in neutral water and require alkali metal ions, protons, or ammonium species for appreciable solubility.<sup>7,17,37</sup> After much experimentation, we settled on 50 mM NaO<sub>2</sub>CCD<sub>3</sub>-buffered D<sub>2</sub>O (pD 4.74) as our common buffer, because it avoids potential issues due to inclusion binding of ammonium buffers in the larger CB[*n*] and is less acidic than the 40% aqueous HCO<sub>2</sub>H employed by Mock.<sup>15</sup>

**Determination of Binding Constants for CB[6].** The majority of host–guest complexes of CB[6] exhibit slow exchange between free and bound guest on the <sup>1</sup>H NMR chemical shift time scale. Consequently, it is possible to measure the concentrations of free and bound host and guest and hence calculate a *K<sub>a</sub>* value from a single <sup>1</sup>H NMR spectrum when the total concentrations of CB[6] and guest are comparable to the *K<sub>d</sub>* value (1/*K<sub>a</sub>*) for the complex.<sup>15</sup> The values of *K<sub>a</sub>* listed for complexes of CB[6] with **7**–**9** and **20** (Table 1) are average values obtained by performing these experiments a minimum of five times at different total concentrations of host and guest.

**Determination of Binding Constants for CB[7].** Relative to CB[6], CB[7] has the ability to include larger guests inside its more spacious cavity. Unfortunately, however, it is not

**Table 1.** Values of *K<sub>a</sub>* (M<sup>−1</sup>) for the Interaction of **1**–**24** with CB[6], CB[7], and CB[8]

	CB[6] (M <sup>−1</sup> )	CB[7] (M <sup>−1</sup> )	CB[8] (M <sup>−1</sup> )
1	— <sup>l</sup>	(2.50 ± 0.39) × 10 <sup>4</sup> <sup>c</sup>	(4.33 ± 1.11) × 10 <sup>11</sup> <sup>k</sup>
2	nb <sup>m</sup>	(4.32 ± 0.68) × 10 <sup>4</sup> <sup>c</sup>	—
3	—	(6.42 ± 1.02) × 10 <sup>4</sup> <sup>c</sup>	(1.11 ± 0.28) × 10 <sup>11</sup> <sup>k</sup>
4	nb	(8.04 ± 1.28) × 10 <sup>4</sup> <sup>c</sup>	—
5	nb	(8.07 ± 0.60) × 10 <sup>4</sup> <sup>c</sup>	—
6	nb	(1.45 ± 0.23) × 10 <sup>5</sup> <sup>c</sup>	—
7	3000 ± 150 <sup>a</sup>	(3.58 ± 0.57) × 10 <sup>5</sup> <sup>c</sup>	—
8	1860 ± 100 <sup>a</sup>	(2.07 ± 0.33) × 10 <sup>6</sup> <sup>c</sup>	—
9	8980 ± 450 <sup>a</sup>	(8.38 ± 1.33) × 10 <sup>6</sup> <sup>c</sup>	—
10	—	(1.32 ± 0.21) × 10 <sup>7</sup> <sup>c,38</sup>	— <sup>39</sup>
11	—	(1.78 ± 0.34) × 10 <sup>7</sup> <sup>e</sup>	(5.78 ± 1.36) × 10 <sup>10</sup> <sup>j</sup>
12	nb	(1.82 ± 0.22) × 10 <sup>7</sup> <sup>d</sup>	nb
13	—	(2.27 ± 0.36) × 10 <sup>7</sup> <sup>c</sup>	—
14	—	(3.81 ± 0.61) × 10 <sup>7</sup> <sup>c</sup>	(6.37 ± 1.20) × 10 <sup>8</sup> <sup>h</sup>
15	nb	(5.18 ± 0.83) × 10 <sup>7</sup> <sup>c</sup>	—
16	(4.49 ± 0.84) × 10 <sup>8</sup> <sup>b</sup>	(8.97 ± 1.43) × 10 <sup>7</sup> <sup>c</sup>	—
17	—	(2.06 ± 0.33) × 10 <sup>8</sup> <sup>c</sup>	—
18	—	(3.23 ± 0.60) × 10 <sup>8</sup> <sup>e</sup>	—
19	nb	(8.88 ± 1.41) × 10 <sup>8</sup> <sup>c</sup>	nb
20	550 ± 30 <sup>a</sup>	(1.84 ± 0.34) × 10 <sup>9</sup> <sup>e</sup>	—
21	—	(3.31 ± 0.62) × 10 <sup>11</sup> <sup>e</sup>	(3.12 ± 0.80) × 10 <sup>9</sup> <sup>k</sup>
22	—	(1.71 ± 0.40) × 10 <sup>12</sup> <sup>g</sup>	(9.70 ± 2.48) × 10 <sup>10</sup> <sup>k</sup>
23	—	(4.23 ± 1.00) × 10 <sup>12</sup> <sup>g</sup>	(8.19 ± 1.75) × 10 <sup>8</sup> <sup>i</sup>
24	—	(1.98 ± 0.42) × 10 <sup>12</sup> <sup>f</sup>	(2.00 ± 0.512) × 10 <sup>9</sup> <sup>k</sup>

<sup>a</sup> Measured directly by <sup>1</sup>H NMR integration of free and bound guest ([CB[6]] = 300 μM). <sup>b</sup> Measured by competition of CB[6] and CB[7] for a limiting quantity of **16**. <sup>c</sup> Measured by competition with **12** for a limiting quantity of CB[7]. <sup>d</sup> Measured by competition with **5** for a limiting quantity of CB[7]. <sup>e</sup> Measured by competition with **19** for a limiting quantity of CB[7]. <sup>f</sup> Measured by competition with **21** for a limiting quantity of CB[7]. <sup>g</sup> Measured by competition with **24** for a limiting quantity of CB[7]. <sup>h</sup> Measured by competition between CB[7], CB[8], and **14**. <sup>i</sup> Measured by competition with **14** for a limiting quantity of CB[8]. <sup>j</sup> Measured by competition with **23** for a limiting quantity of CB[8]. <sup>k</sup> Measured by competition with **11** for a limiting quantity of CB[8]. <sup>l</sup> — = not determined. <sup>m</sup> nb = no inclusion binding detected by <sup>1</sup>H NMR.

generally possible to determine values of *K<sub>a</sub>* for CB[7]·guest complexes by direct NMR measurements, because they exceed the experimentally accessible range (up to ≈10<sup>4</sup> M<sup>−1</sup>) and more commonly display fast exchange kinetics relative to the NMR chemical shift time scale. We therefore, resorted to the indirect method based on <sup>1</sup>H NMR spectroscopy introduced by Mock in his pioneering work on CB[6].<sup>15</sup> In our implementation of this method a tight binding guest that exhibits slow exchange kinetics and an excess of a more weakly binding guest are allowed to compete for a limiting quantity of CB[7]. The concentration of the weaker guest is adjusted until the more tightly binding guest is approximately 50% bound; integration of the resonances for the free and bound guest then allow for a calculation of a relative binding constant (*K<sub>rel</sub>*). These *K<sub>rel</sub>* values can be converted to absolute binding constants (*K<sub>a</sub>*) provided that a reference guest is available for which *K<sub>a</sub>* is known accurately.

As a reference guest for the CB[7] binding constants presented in Table 1, we selected 1,3-diaminobenzene (**5**), the absolute *K<sub>a</sub>* of which could be determined accurately by UV/vis titration. Figure 1a shows UV/vis spectra recorded during the titration of a fixed concentration of **5** with CB[7]. Figure 1b shows a plot of the absorbance at 231 nm as a function of total CB[7] concentration and the best fit to a 1:1 binding model with *K<sub>a</sub>* = 8.07 ± 0.60 × 10<sup>4</sup> M<sup>−1</sup>. The presence of isosbestic points at 238 and 291 nm establishes that this system undergoes a clean two-state equilibrium that is critical if CB[7]·**5** is to be used as a reference *K<sub>a</sub>*.

- (31) The CB[*n*] family exhibits unusual kinetics of association and dissociation in addition to its remarkable thermodynamic properties.  
 (32) Ong, W.; Gomez-Kaifer, M.; Kaifer, A. E. *Org. Lett.* **2002**, *4*, 1791–1794.  
 (33) Ong, W.; Kaifer, A. E. *Organometallics* **2003**, *22*, 4181–4183.  
 (34) Fu, H.-Y.; Xue, S.-F.; Zhu, Q.-J.; Tao, Z.; Zhang, J.-X.; Day, A. I. *J. Inclusion Phenom. Macrocycl. Chem.* **2005**, *52*, 101–107. Cong, H.; Yang, F.; Tao, Z.; Zhang, J.-X. *Wuji Huaxue Xuebao* **2005**, *21*, 349–356. Dai, L.-P.; Tao, Z.; Zhu, Q.-J.; Xue, S.-F.; Zhang, J.-X.; Zhou, X. *Huaxue Xuebao* **2004**, *62*, 2431–2440.  
 (35) Seino, H.; Mochizuki, A.; Ueda, M. *J. Polym. Sci., Part A: Polym. Chem.* **1999**, *37*, 3584–3590.  
 (36) Zhang, W.; Simanek, E. E. *Org. Lett.* **2000**, *2*, 843–845.  
 (37) Buschmann, H.-J.; Cleve, E.; Jansen, K.; Wego, A.; Schollmeyer, E. *Mater. Sci. Eng., C* **2001**, *C14*, 35–39. Zhang, G.-L.; Xu, Z.-Q.; Xue, S.-F.; Zhu, Q.-J.; Tao, Z. *Wuji Huaxue Xuebao* **2003**, *19*, 655–659.



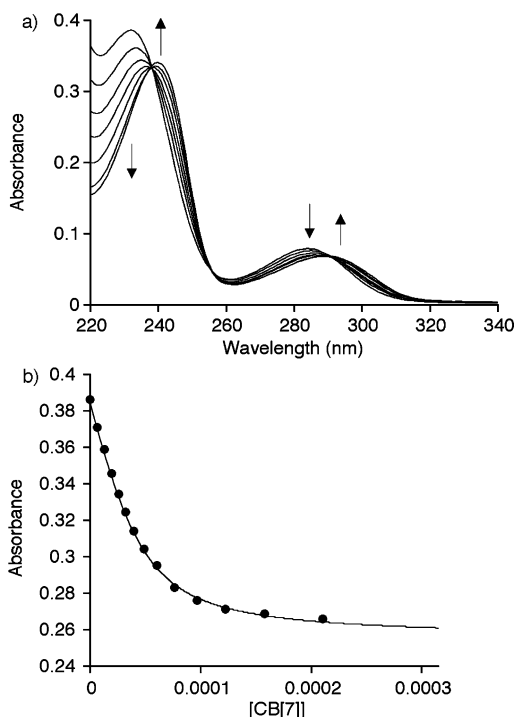


**Figure 1.** (a) Selected UV/vis spectra from the titration of **5** ( $44 \mu\text{M}$ ) with CB[7] ( $0\text{--}210 \mu\text{M}$ ). (b) Plot of the absorbance for **5** ( $231 \text{ nm}$ ) as a function of total CB[7] concentration. The solid line represents the best least-squares fit of the data to a 1:1 binding model ( $K_a = 80\,700 \pm 6000 \text{ M}^{-1}$ ).

We fortuitously discovered that the common internal reference used for  $^1\text{H}$  NMR in water, TMSP (**12**), and its relative **19** bind tightly to CB[7], exhibiting slow exchange kinetics on the chemical shift time scale with resonances in the uncluttered 0 to  $-1$  ppm region of the spectrum, which minimizes the errors associated with spectral integration that facilitated our studies.<sup>40</sup> For example, Figure 2 shows the  $^1\text{H}$  NMR spectra that were obtained when **19** and **20** were allowed to compete for CB[7] along with reference spectra for the various components. In this way, the values of  $K_a$  for a variety of CB[7] complexes (CB[7]·**1**–CB[7]·**24**) were determined (Table 1).

**Determination of Binding Constants for CB[8].** The implementation of the  $^1\text{H}$  NMR competition method for the determination of the relative binding constants for CB[8] was challenging for several reasons. Although many of the amines used in this study bind to CB[8] (e.g. **10**, **13**, and **23**) most display intermediate exchange kinetics on the chemical shift time scale. Furthermore, the slimmer guests (e.g. **8**, **13**, or **20**) may bind with either 1:1 or 1:2 CB[8]:guest stoichiometry.<sup>41</sup> Last, the guests that undergo UV/vis changes upon complexation (e.g. **10** and **14**) have values of  $K_a$  that exceed the range that is accurately determined by this technique ( $K_a > 10^6 \text{ M}^{-1}$ ) in our buffer.<sup>42</sup> To circumvent these issues, we utilized the complexes

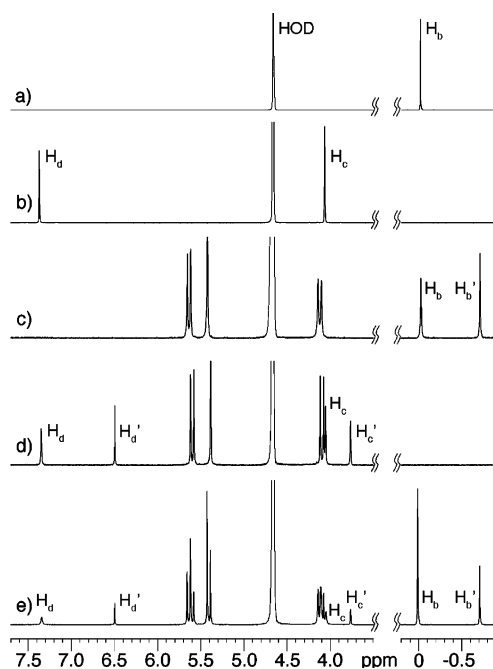


**Figure 2.** A portion of the  $^1\text{H}$  NMR spectra ( $400 \text{ MHz}$ ,  $298 \text{ K}$ ,  $50 \text{ mM NaO}_2\text{CCD}_3$  buffer,  $\text{pD } 4.74$ ) recorded for (A) **19**, (B) **20**, (C) a mixture of **19** and CB[7]·**19**, (D) a mixture of **20** and CB[7]·**20**, and (E) a mixture of CB[7], **19** ( $2 \text{ equiv}$ ), and **20** ( $1 \text{ equiv}$ ).  $[\text{CB}[7]]_{\text{Total}} = 500 \mu\text{M}$ . The resonances for  $\text{H}_a$  and  $\text{H}_a'$  fall in the  $2.5\text{--}1.5$  ppm region. Primed and unprimed resonances refer to bound and free guest, respectively.

CB[7]·**14** and CB[8]·**14** recently reported by Kaifer, both of which show slow exchange on the NMR chemical shift time scale.<sup>24,43</sup> We allowed CB[7] and CB[8] to compete for a limiting quantity of **14**, which allowed us to calculate  $K_a = 6.4 \times 10^8 \text{ M}^{-1}$  for CB[8]·**14**. Competition experiments then allowed the determination of the affinity of the CB[8]·**11** complex ( $K_a = 5.78 \times 10^{10} \text{ M}^{-1}$ ), which displayed tight binding and slow kinetics of exchange on the chemical shift time scale. For example, Figure 3 shows the NMR spectra recorded for the competition between **3** and **11** for CB[8]. The  $-\text{NMe}_3^+$  groups of **3** and the aromatic protons of **11** both show significant upfield shifts and slow exchange in the  $^1\text{H}$  NMR spectra of their CB[8] complexes. In practice, however, it is more straightforward to monitor free and bound **11**, since its aromatic resonances appear in a relatively uncluttered region ( $7.5\text{--}6.0$  ppm) of the  $^1\text{H}$  NMR spectrum. The CB[8]·**11** complex was then used to determine  $K_a$  values for the remaining CB[8] complexes (Table 1).

## Discussion

**X-ray Crystal Structures of CB[8]·**3** and CB[8]·**11**.** Figure 4 shows the X-ray crystal structure obtained for CB[8]·**3**. Compound **3** with its large trimethylammonium substituents is complementary in size and shape to the cavity of CB[8]. Interestingly, **3** is not symmetrically situated in the cavity of CB[8]; one of the  $-\text{NMe}_3^+$  groups resides within the cavity,

(38) Kim and Kaifer previously reported (ref 26 and 32) the  $K_a$  for CB[7]·**10** [ $(1\text{--}2) \times 10^8 \text{ M}^{-1}$ ] in  $0.2 \text{ M NaCl}$  and  $50 \text{ mM Tris}$  buffer. The larger value of  $K_a$  measured here probably reflects buffer and pH effects.

(39) Kim previously reported (ref 52) the  $K_a$  for the 1:1 complex CB[8]·**10** as  $110\,000 \text{ M}^{-1}$  in water.

(40) We determined the  $T_1$  values for guest and host–guest complex by the standard inversion recovery sequence. For  $K_a$  determinations, we used a delay time of 5 times the longest  $T_1$  to avoid systematic integration errors due to incomplete relaxation.

(41) We have specifically avoided the determination of CB[8]:guest binding constants in cases where the possibility of 1:2 binding exists.  $K_{\text{rel}}$  determinations using the methodology described in this paper are not applicable in such situations.

(42) Although  $K_a$  determinations were possible in more competitive buffers (refs 24 and 43), we were not able to determine  $K_a$  values for the CB[7]·**14** or CB[8]·**14** complexes by direct UV/vis and fluorescence titrations in our buffer. It is well-known that CB[6] and CB[7] competitively bind alkali metal ions and/or protons at their ureidyl-carbonyl portals, which reduces the observed values of  $K_a$ . At the fixed concentrations of **14** required for accurate titration ( $1/K_a$ ;  $26 \text{ nM}$  for CB[7] and  $1.5 \text{ nM}$  for CB[8]), we were not able to achieve a stable signal on our fluorometer.

(43) Sindelar, V.; Cejas, M. A.; Raymo, F. M.; Chen, W.; Parker, S. E.; Kaifer, A. E. *Chem. Eur. J.* **2005**, *11*, DOI: 10.1002/chem.200500917.

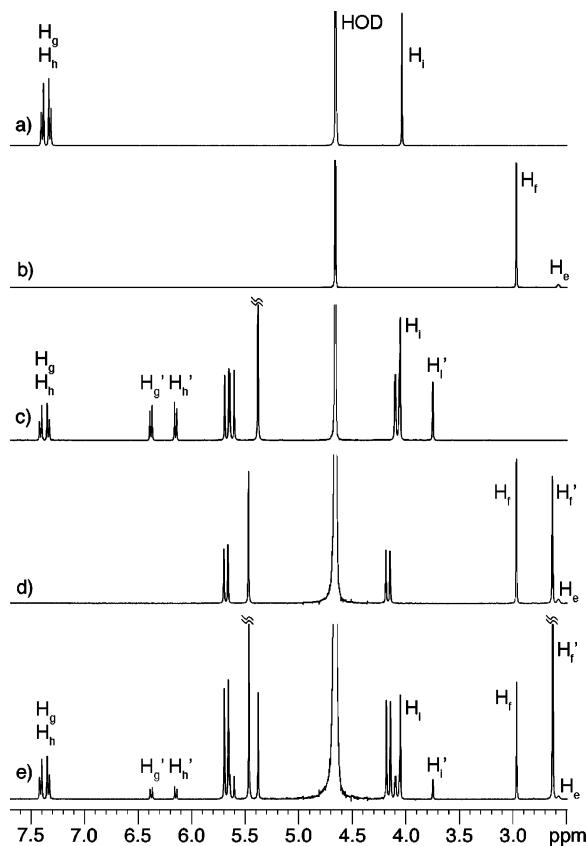


**Figure 3.** A portion of the  $^1\text{H}$  NMR spectra (400 MHz, 298 K, 50 mM  $\text{NaO}_2\text{CCD}_3$  buffer, pD 4.74) recorded for (A) **11**, (B) **3**, (C) a 1:1 mixture of **11** and  $\text{CB}[8]\cdot\mathbf{11}$ , (D) a 1:1 mixture of **3** and  $\text{CB}[8]\cdot\mathbf{3}$ , and (E) a mixture of  $\text{CB}[8]$ , **3** (1 equiv), and **11** (2 equiv).  $[\text{CB}[8]]_{\text{Total}} = 320 \mu\text{M}$ . The unlabeled protons of **3** resonate upfield (2.1–0.9 ppm). Primed and unprimed resonances refer to bound and free guest, respectively.

whereas the other is located externally. In contrast, the  $^1\text{H}$  NMR spectrum of  $\text{CB}[8]\cdot\mathbf{3}$  indicates that the two  $-\text{NMe}_3^+$  groups are equivalent on the NMR chemical shift time scale. In solution it is possible that  $\text{CB}[8]\cdot\mathbf{3}$  undergoes rapid interconversion between two equivalent conformations of the type indicated in Figure 4a or that a symmetrical conformation is preferred. One interesting aspect of the X-ray structure of  $\text{CB}[8]\cdot\mathbf{3}$  is the observed ellipsoidal deformation.<sup>44</sup> We quantify this deformation by measurement of the length of short and long axes of this ellipsoid at the equator (short, 12.3 Å; long, 13.7 Å) and at the carbonyl portals (short, 9.20 Å; long, 10.5 Å). This structural change is not due to a gross change in the geometry of the glycoluril subunits, which maintain the  $\text{O}\cdots\text{O}$  separation (6.00–6.16 Å) typically observed for uncomplexed  $\text{CB}[n]$ , but rather is due to a splaying of the connecting methylene bridges. A second unusual aspect of the crystal structure of  $\text{CB}[8]\cdot\mathbf{3}$  relates to the packing of these molecules within the crystal (Figure 4b). The  $\text{CB}[8]\cdot\mathbf{3}$  complexes assume a close-packed arrangement, resulting in a sheetlike structure. These sheets are stacked in the crystal such that each  $\text{CB}[8]\cdot\mathbf{3}$  is *in register* with the one below it. This registration between layers results in infinite guest-filled channels within the crystal. The interstitial channels between the  $\text{CB}[8]$  macrocycles are filled with the iodide counterions that accompany **3**. Figure 4c shows the crystal structure of  $\text{CB}[8]\cdot\mathbf{11}$ , which demonstrates the 1:1 nature of the

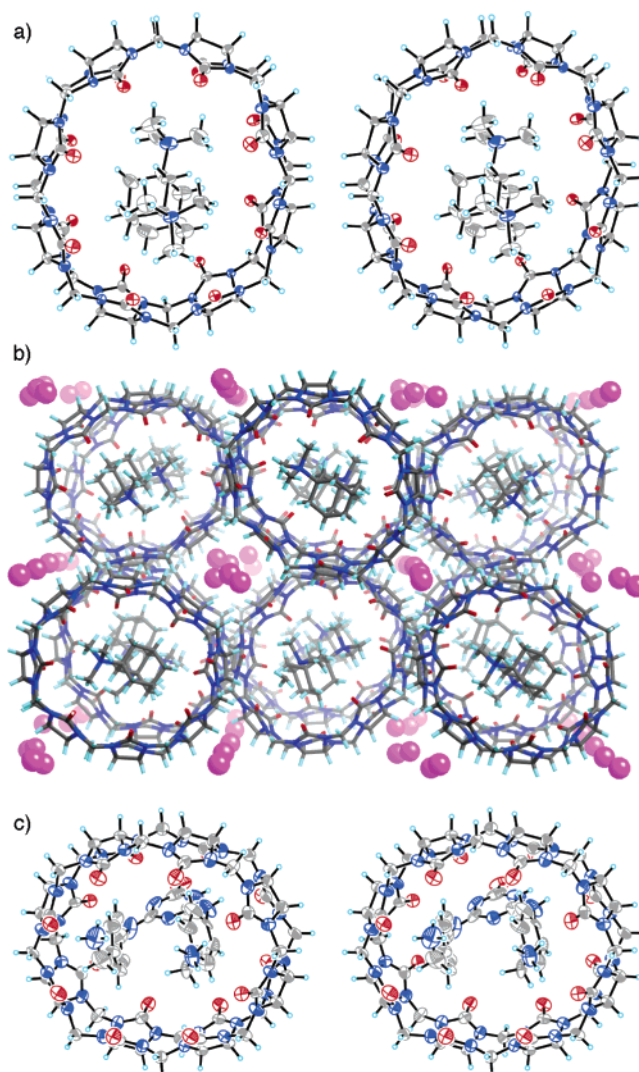


**Figure 4.** (a) Cross-eyed stereoview of the  $\text{CB}[8]\cdot\mathbf{3}$  complex in the crystal. (b) Rendering of the crystal packing observed for  $\text{CB}[8]\cdot\mathbf{3}$ . (c) Cross-eyed stereoview of the  $\text{CB}[8]\cdot\mathbf{11}$  complex in the crystal. Thermal ellipsoids are drawn at the 50% probability level. Atom colors: C, gray; N, blue; O, red; H, aqua; I, purple.

complex and the U-shaped geometry adopted by **11** within the complex. Complex  $\text{CB}[8]\cdot\mathbf{11}$  also exhibits an ellipsoidal deformation. The packing of  $\text{CB}[8]\cdot\mathbf{11}$  in the crystal is similar to that of  $\text{CB}[8]\cdot\mathbf{3}$  with infinite guest-filled channels defined by  $\text{CB}[8]$  macrocycles along with interstitial channels occupied by iodide counterions used during crystallization.

**Guest Affinity Toward  $\text{CB}[6]$ ,  $\text{CB}[7]$ , and  $\text{CB}[8]$ .** The pioneering work of Mock<sup>15</sup> has clearly delineated the importance of size and shape complementarity as well as the importance of ion–dipole interactions in the formation of  $\text{CB}[6]$  complexes. Consequently, we measured the affinities of  $\text{CB}[6]$  toward a small number of guests in pD 4.74  $\text{NaO}_2\text{CCD}_3$  buffer and observed binding affinities and trends similar to those reported by Mock.<sup>15</sup> For example, *p*-toluidine **9** binds with modest affinity ( $K_a = 8980 \text{ M}^{-1}$ ), whereas the slimmer, dicationic guest **16** binds much more strongly ( $K_a = 4.49 \times 10^8 \text{ M}^{-1}$ ). These  $K_a$  values are slightly larger than those reported by Mock ( $\text{CB}[6]\cdot\mathbf{9}$ ,  $K_a = 1265 \text{ M}^{-1}$ ;  $\text{CB}[6]\cdot\mathbf{16}$ ,  $K_a = 2.8 \times 10^6 \text{ M}^{-1}$ ); we attribute this difference to the more competitive medium (1:1  $\text{H}_2\text{O}:\text{HCO}_2\text{H}$ ) and higher temperature (40 °C) employed by Mock.

(44) Samsonenko, D. G.; Virovets, A. V.; Lipkowski, J.; Geras'ko, O. A.; Fedin, V. P. *J. Struct. Chem.* **2002**, *43*, 664–668.

Given the similarity in structure between CB[6], CB[7], and CB[8], it is reasonable to hypothesize that the importance of size, shape, length, and electrostatic complementarity will transfer from CB[6] to the higher homologues. The three isomeric diaminobenzenes (**4**, **5**, and **8**) illustrate that the influence of guest shape transfers from CB[6] to CB[7]. For example the ortho- and meta-substituted compounds (**4** and **5**) form CB[7] complexes of modest affinity ( $K_a \approx 8 \times 10^4 \text{ M}^{-1}$ ), whereas the para-substituted species (**8**) binds 26-fold tighter. CB[7] also appears to retain much of the length and functional group preference of CB[6]. In this regard, it is interesting to consider para-disubstituted guests **8**, **9**, and **15**, which differ in the nature (e.g.  $\text{NH}_3^+$ ,  $\text{CH}_3$ , and  $\text{SMe}_2^+$ ) and number of cationic substituents. Compound **8** displays the lowest affinity toward CB[7] due to the distance mismatch between the two  $\text{NH}_3^+$  groups of **8** and the ureidyl-carbonyl portals of CB[7]. Despite the difference in charge between **8** and **9**, **9** binds 4-fold tighter to CB[7], presumably due to positioning of the  $\text{CH}_3$  group nearer the hydrophobic interior of CB[7]. Sulfonium salt **15** binds 6-fold tighter than ammonium ion **9** probably due to differences in aqueous solvation between the free guests. CB[7] also displays a strong preference for appropriately sized guests. Accordingly, the slightly wider cyclohexanediamine **13** binds 11-fold tighter to CB[7] than does phenylenediamine **8**.

It is known from the work of Kim that the adamantane skeleton is complementary to the cavity of CB[7];<sup>7</sup> herein, we have studied the binding properties of CB[7] toward seven mono-, di-, and trisubstituted adamantanes to further probe the size limits and functional group preferences of CB[7]. For example, among the monosubstituted compounds, CB[7] displays a  $10^4$ -fold preference for the cationic ammonium species (**22**, **23**, and **24**) relative to **18**. The nature of the ammonium species (e.g. quaternary, pyridinium,  $\text{NH}_3^+$ ) is relatively unimportant. Despite a common  $\text{N}\cdots\text{N}$  distance and charge, disubstituted adamantanes **3** and **17** form CB[7] complexes of remarkably different affinity (3200-fold). The reason is straightforward and instructive; the size of **3** with its bulky  $\text{NMe}_3^+$  groups exceeds the cavity volume of CB[7] and forms only an exclusion complex. Remarkably, trisubstituted adamantane **1** forms a weak inclusion complex with CB[7] ( $K_a = 2.50 \times 10^4 \text{ M}^{-1}$ ) that is in slow exchange on the chemical shift time scale. Molecular modeling (MMFF) suggests that unfavorable steric interactions between one of the  $\text{CH}_3$  groups and the wall of CB[7] build up in the complex (Figure 5a). Even more remarkable than the high selectivity displayed by CB[7] is the magnitude of the CB[7]·**23** binding constant ( $K_a = 4.23 \times 10^{12} \text{ M}^{-1}$ ,  $\Delta G = -17.2 \text{ kcal mol}^{-1}$ ), which places it among the tightest noncovalent synthetic host–guest pairs known to date.<sup>46</sup>

During the course of our investigations, we made several other observations that deserve comment. First, we found that guests containing trimethylsilyl groups undergo strong complexation with CB[7] (e.g. CB[7]·**12**,  $K_a = 1.82 \times 10^7 \text{ M}^{-1}$ ; CB[7]·**19**,  $K_a = 8.88 \times 10^8 \text{ M}^{-1}$ ). Figure 5b shows an MMFF-minimized model of the CB[7]·**19** complex that illustrates the excellent match between the size and shape of the  $\text{Me}_3\text{Si}$  substituent and

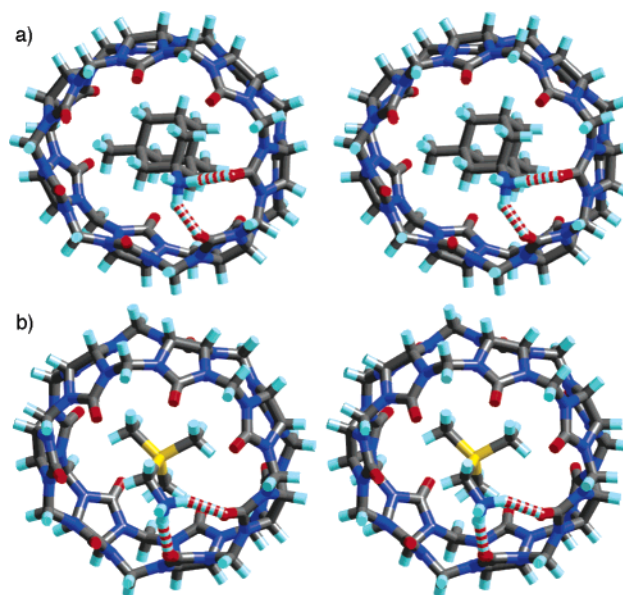


**Figure 5.** Cross-eyed stereoviews of the MMFF-minimized structures of (a) CB[7]·**1** and (b) CB[7]·**19**. Atom colors: C, gray; N, blue; O, red; H, aqua; Si, yellow; H-bonds, red–aqua striped.

the cavity of CB[7]. In accord with literature precedent, we find that **10**,<sup>26,32</sup> **14**,<sup>24</sup> and **21**<sup>45</sup> form tight complexes with CB[7]. Compound **11** by virtue of its two *p*-aminobenzylamine substituents is theoretically capable of forming complexes of different CB[7]:**11** stoichiometry (e.g. 1:1 or 2:1). At millimolar concentrations, we observe the exclusive formation of the 1:1 complex CB[7]·**11**, even when CB[7] is present in excess. Molecular modeling (MMFF) suggests that the CB[7]·**11** complex assumes a geometry (Supporting Information) where the second *p*-aminobenzylamine substituent is sterically excluded from complexation. A final interesting aspect of CB[7] recognition behavior that deserves comment is the destabilizing influence of a negative charge adjacent to the carbonyl portal on CB[7] complex stability, which was recently reported by Kim, Kaifer, Inoue and co-workers<sup>45</sup> We believe the high affinity observed for CB[7] binding to carboxylic acid based guests **6**, **12**, and **18** in this study reflects the fact that we work under acidic conditions, where the  $\text{CO}_2\text{H}$  groups are predominantly protonated and uncharged within their CB[7] complexes.

The use of the  $^1\text{H}$  NMR competition method for our  $K_a$  determinations limits us to studies of complexes that form 1:1 complexes exclusively. To ensure the exclusive formation of 1:1 complexes, even under conditions where one component is present in (large) excess, we restrict our studies to compounds (mainly adamantanes) that completely fill the cavity of CB[8]. Accordingly, the values of  $K_a$  measured for these complexes are large ( $K_a > 10^8 \text{ M}^{-1}$ ) and do not span as large a range of free energies as those determined for CB[7].

The CB[8]·**11** complex, which was used for the majority of the CB[8] competition experiments, displays several unusual features. For example, although free **11** populates three different rotamers, complexation within CB[8] induces a folding process resulting in the U-shaped CB[8]·**11** complex (Figure 4c).<sup>47,48</sup> To provide strong evidence for the formation of a 1:1 CB[8]·

(45) Jeon, W. S.; Moon, K.; Park, S. H.; Chun, H.; Ko, Y. H.; Lee, J. Y.; Lee, E. S.; Samal, S.; Selvapalam, N.; Rekharsky, M. V.; Sindelar, V.; Sobransingh, D.; Inoue, Y.; Kaifer, A. E.; Kim, K. *J. Am. Chem. Soc.* **2005**, *127*, 12984–12989.

(46) Houk, K. N.; Leach, A. G.; Kim, S. P.; Zhang, X. *Angew. Chem., Int. Ed.* **2003**, *42*, 4872–4897. Rao, J.; Lahiri, J.; Isaacs, L.; Weis, R. W.; Whitesides, G. M. *Science* **1998**, *280*, 708–711.

(47) Jeon, W. S.; Ziganshina, A. Y.; Lee, J. W.; Ko, Y. H.; Kang, J.-K.; Lee, C.; Kim, K. *Angew. Chem., Int. Ed.* **2003**, *42*, 4097–4100.

(48) Jeon, W. S.; Kim, E.; Ko, Y. H.; Hwang, I.; Lee, J. W.; Kim, S.-Y.; Kim, H.-J.; Kim, K. *Angew. Chem., Int. Ed.* **2005**, *44*, 87–91.



**11** complex in solution, we measured its diffusion coefficient ( $D = 2.52 \times 10^{-10} \text{ m}^2 \text{ s}^{-1}$ ) by DOSY NMR.<sup>49</sup> The value measured for CB[8]·**11** is quite similar to that measured for the known 1:1 complex CB[8]·**3** ( $D = 2.60 \times 10^{-10} \text{ m}^2 \text{ s}^{-1}$ ) as an internal standard, which allows us to conclude that CB[8]·**11** is also a 1:1 complex.<sup>50</sup> The rate of dissociation of **11** from the CB[8]·**11** complex is uncommonly slow (half-life  $\approx 1$  d). We hypothesize that **11** must undergo an unfolding process within the CB[8]·**11** complex before it can exit CB[8], which would impose a large (steric) barrier to dissociation.

Although we have determined only a limited number of  $K_a$  values for CB[8] complexes, we can discern several trends in its binding behavior. For example, adamantane carboxylic acid (**18**) forms a weak complex with CB[8], whereas adamantaneamine (**23**) forms a tight complex ( $K_a = 8.19 \times 10^8 \text{ M}^{-1}$ ). Positively charged substituents promote complexation within CB[8] due to the presence of cation–dipole interactions that have been implicated in the binding properties of CB[6].<sup>15</sup> It is tempting to directly compare the values of  $K_a$  for monosubstituted adamantanes **22–24** and conclude that CB[8] prefers quaternary ammonium species (**22**) relative to pyridinium (**24**) or ammonium (**23**) ions. We believe, however, that a substantial portion of the 49-fold preference of CB[8] for **22** is due to differences in size and shape that result from partial inclusion of its  $-\text{NMe}_3^+$  substituent in the cavity of CB[8]. This interpretation is supported by the X-ray crystal structure of CB[8]·**3** (Figure 4a) and by the large preference of CB[8] for **1** relative to **23** (529-fold). Compound **1** with its two additional Me groups more effectively fills the cavity of CB[8] relative to **23** while  $\text{NH}_3^+$  cation–dipole interactions are maintained. Similarly, compound **3** binds to CB[8] with comparable affinity to **22**, despite the presence of two  $-\text{NMe}_3^+$  substituents. This result suggests that size and shape complementarity may assume more important roles in the complexation behavior of the larger CB[ $n$ ] as their portal regions expand. As expected on the basis of literature precedent, CB[8] also forms a tight complex with ferrocene derivative **21**.<sup>45</sup> On the basis of this admittedly limited data set, it appears that CB[8] retains many of the outstanding properties typically associated with CB[6] complexes (e.g., high affinity; high selectivity due to well-defined size, shape, and functional group preferences; and some of the unusual dynamic aspects of guest inclusion and dissociation).

**Guest Selectivity among CB[6], CB[7], and CB[8].** The previous sections establish that many of the trends seen in the complexation behavior of CB[6] also apply to CB[7] and CB[8] *considered individually*. Such high affinity and selectivity in aqueous recognition processes of a single host are preceded but unusual in synthetic systems. In sharp contrast, nature's recognition platforms (e.g. proteins, antibodies, nucleic acids) display high selectivity and affinity not only individually but also collectively. The web of self-sorting reaction and interaction networks that characterize natural systems ultimately give rise to the emergent processes that embody life processes. In this section we present the CB[ $n$ ] family as the first class of synthetic hosts with sufficient affinity and selectivity *considered collectively* to serve as components of complex self-sorting systems

that enable them to mimic some of the complexity seen in natural systems.

Consider, for example, the complexation behavior of CB[6], CB[7], and CB[8] toward **1**. Compound **1** is excluded from the cavity of CB[6], weakly included within CB[7] ( $K_a = 2.50 \times 10^4 \text{ M}^{-1}$ ), but binds with picomolar affinity to CB[8] ( $K_a = 4.33 \times 10^{11} \text{ M}^{-1}$ )! Such levels of selectivity across a homologous series of synthetic hosts is remarkable. Compound **3** displays a similar binding profile. Such processes may seem contrived in that **1** and **3** only bind tightly to CB[8], the cavity volume of which they do not exceed. In that regard, consider the behavior of **23**, which is excluded from CB[6] but prefers CB[7] over CB[8] more than 5000-fold. We suggest that this extraordinarily high selectivity is due to a nearly ideal size match between the adamantane core of **23** and CB[7]. Similarly, compounds **12** and **19** with their  $\text{Me}_3\text{Si}$  groups form tight inclusion complexes with CB[7] but are excluded from CB[6] and CB[8]. Or even more interestingly, consider the behavior of compound **11**, which contains two identical binding epitopes. Compound **11** binds 3250-fold more tightly to CB[8] than CB[7] and additionally acts as a conformational control element, resulting in exclusive population of the U-shaped rotamer. This result suggests that CB[8] may be used as an allosteric regulator of binding and potentially catalysis in complex self-sorting systems in much the same way as nature uses small molecules to regulate protein function. The results presented here, in combination with those from other groups, have demonstrated the unique kinetics of complexation and dissociation of CB[ $n$ ],<sup>19,21,51</sup> their ability to respond to external stimuli (e.g. light and electrochemistry),<sup>25,27,30,32,33,48,52</sup> as well as their ability to accelerate and control reactions, suggesting that the CB[ $n$ ] family is uniquely suited for applications as components of complex self-sorting systems,<sup>1–3</sup> including molecular machines and biomimetic systems.

## Conclusions

We have used  $^1\text{H}$  NMR competition experiments to measure values of  $K_{\text{rel}}$  for CB[6], CB[7], and CB[8] toward a variety of guests referenced to an absolute  $K_a$  determined by UV/vis measurements. We find that the larger CB[ $n$ ] homologues, CB[7] and CB[8], *individually* retain much of the remarkable binding characteristics usually associated with CB[6] complexes, namely high levels of affinity and selectivity based on guest size, shape, length, and chemical functionality. The cavity of CB[7] is complementary to trimethylsilyl groups (e.g. **12** and **19**) and exhibits remarkable affinity toward adamantane derivatives (e.g. **22–24**) with values of  $K_a$  exceeding  $10^{12} \text{ M}^{-1}$  (femtomolar  $K_d$ !), placing them among the tightest synthetic host–guest pairs known. The X-ray crystal structure of CB[8]·**11** demonstrates the excellent fit between the U-shaped conformer of **11** and the cavity of CB[8]. The CB[8]·**11** complex is unusual in that it exhibits slow dissociation kinetics (half-life  $\approx 1$  d); we attribute this result to a need for **11** to assume an unfolded conformation before dissociation can occur. This result suggests a strategy to control rate constants—the introduction of conformational changes required for association or dissociation—that can be used in much the same way that supramolecular chemistry now uses the complementarity of interacting surfaces to control binding affinity.

(49) Cohen, Y.; Avram, L.; Frish, L. *Angew. Chem., Int. Ed.* **2005**, *44*, 520–554.

(50)  $^1\text{H}$  NMR integration alone did not allow us to differentiate between complexes with the same relative stoichiometry (e.g., 1:1 vs 2:2 vs  $n:n$ ).

(51) Hoffmann, R.; Knoche, W.; Fenn, C.; Buschmann, H.-J. *J. Chem. Soc., Faraday Trans.* **1994**, *90*, 1507–1511.



Even more remarkable than the observation that CB[7] and CB[8] preserve much of the binding profile of CB[6] is the observation of the high levels of selectivity exhibited by the CB[*n*] family considered *collectively*, that is, the differences in  $K_a$  observed for complexes of a common guest with CB[6], CB[7], and CB[8]. For example, CB[7] exhibits high selectivity for adamantane guests (e.g., **23**, 5100-fold; **24**, 990-fold) relative to the corresponding CB[8] complexes. When the guest exceeds the binding capacity of the host, even larger levels of selectivity are observed. For example, guests **1** and **3**, and **11** prefer CB[8] relative to CB[7] by factors greater than  $10^7$  and  $10^6$ , respectively. Such high levels of affinity and selectivity, particularly for recognition processes in aqueous solution, are unprecedented across a synthetic host family. These high levels of affinity and selectivity—hallmarks of biological systems—suggest that members of the CB[*n*] family are prime components for the preparation of complex self-sorting systems.<sup>1,2</sup> The high levels of selectivity ( $K_{rel}$ ) observed for CB[*n*] complexes *individually and collectively* translates to differences in free energy ( $\Delta G$ ) that can be used to control the behavior of complex systems as they proceed toward thermodynamic equilibrium. Nature uses such differences in free energy, along with catalysis and compartmentalization, as one of the chemical fuels for the remarkable emergent behaviors displayed by living systems (e.g. controlled motion, reproduction, sensing, and self-defense). On the basis of this analysis, we suggest that the CB[*n*] family is uniquely positioned to serve as components of complex self-sorting systems that display a variety of biomimetic functions.

## Experimental Section

Starting materials were purchased from Alfa-Aesar, Acros, and Aldrich and were used without further purification. CB[6], CB[7] and CB[8] were prepared according to a literature procedure.<sup>10</sup> Compounds **1**, **2**, **4–10**, **12**, **13**, **16**, and **18–24** were commercially available. Compounds **15**,<sup>53</sup> **17**,<sup>35</sup> and **25**<sup>36</sup> were prepared by literature procedures. TLC analysis was performed using precoated glass plates from E. Merck. Column chromatography was performed using silica gel (230–400 mesh, 0.040–0.063  $\mu\text{m}$ ) from E. Merck using eluents in the indicated v:v ratio. Melting points were measured on a Meltemp apparatus in open capillary tubes and are uncorrected. IR spectra were recorded on a Nicolet Magna spectrophotometer as KBr pellets or thin films on NaCl plates and are reported in  $\text{cm}^{-1}$ . NMR spectra were measured on Bruker AM-400 and DRX-400 instruments operating at 400 MHz for  $^1\text{H}$  and 100 MHz for  $^{13}\text{C}$ . Mass spectrometry was performed using a VG 7070E magnetic sector instrument by fast atom bombardment (FAB) using the indicated matrix or on a JEOL AccuTOF electrospray instrument. The matrix “magic bullet” is a 5:1 (w:w) mixture of dithiothreitol:dithioerythritol.

**Compound 3.** A mixture of **17** (0.050 g, 0.21 mmol), MeI (0.17 mL, 2.66 mmol), and  $\text{NaHCO}_3$  (0.175 g, 2.08 mmol) in MeOH (5 mL) was heated at reflux for 72 h. The reaction mixture was concentrated by rotary evaporation and dried under high vacuum for 1 h. The product was washed with hot  $\text{CH}_3\text{COCH}_3$  (50 mL) and then dissolved in hot  $\text{CH}_3\text{CN}$  (25 mL). After a few hours, compound **3** was obtained as a microcrystalline solid by filtration (0.090 g, 0.18 mmol, 86%). Mp: 252 °C. IR (KBr,  $\text{cm}^{-1}$ ): 3029w, 3009w, 2963w, 2924w, 2858w, 1623m, 1487m, 1456w, 1417w, 1379w, 1347w, 1118m, 1071m, 1037m.  $^1\text{H}$  NMR (400 MHz,  $\text{D}_2\text{O}$ ): 3.13 (s, 18H), 2.74 (br., 2H), 2.36 (s, 2H), 2.12 (br. m, 8H), 1.68 (br., 2H).  $^{13}\text{C}$  NMR (100 MHz,  $\text{D}_2\text{O}$ ): 74.6,

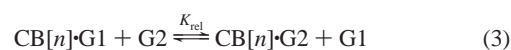
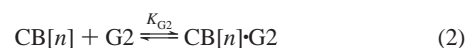
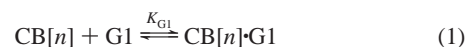
49.4, 33.2, 33.1, 32.8, 30.9. MS (FAB, magic bullet):  $m/z$  379 (100,  $[\text{M} - \text{I}]^+$ ). HR-MS (FAB, magic bullet):  $m/z$  379.1602 ( $[\text{M} - \text{I}]^+$ ,  $\text{C}_{16}\text{H}_{32}\text{N}_2\text{I}$ , calcd 379.1610).

**Compound 11.** Compound **25** (300 mg, 0.54 mmol) was dissolved in a mixture of TFA (3 mL) and  $\text{H}_2\text{O}$  (5 mL) and heated at 85 °C for 10 h. The reaction mixture was cooled to room temperature and then placed in the refrigerator for 1 d. The small, needlelike crystals that formed were isolated by filtration and dried on the frit overnight, yielding **11** (290 mg, 0.51 mmol, 95%) as a white solid. Mp: >300 °C. IR (KBr,  $\text{cm}^{-1}$ ): 2890m, 1732s, 1685s, 1594m, 1501s, 1365s, 1211s, 1178m, 1140m.  $^1\text{H}$  NMR (400 MHz,  $\text{D}_2\text{O}$ ): 7.51 (br. s, 8H), 4.21 (s, 4H).  $^{13}\text{C}$  NMR (100 MHz,  $\text{D}_2\text{O}$ ): 163.20 (q,  $^2J_{\text{CF}} = 36$  Hz), 157.20, 151.16, 136.13, 132.52, 130.58, 125.66, 117.34 (q,  $^1J_{\text{CF}} = 292$  Hz), 43.48. ES-MS:  $m/z$  338 (100,  $[\text{M} - \text{H} - 2\text{CF}_3\text{CO}_2]^+$ ). HR-MS (ES-MS):  $m/z$  338.1737 ( $[\text{M} - \text{H} - 2\text{CF}_3\text{CO}_2]^+$ ,  $\text{C}_{17}\text{H}_{20}\text{N}_7\text{O}$ , calcd 338.1729).

**Computations.** The minimizations reported in this paper were performed with Spartan 02 running on a PowerMac G4.

**UV/Vis Titrations.** UV/vis spectra were recorded on a Perkin-Elmer double-beam spectrophotometer using 1-cm path length cells. A series of spectra were obtained by the addition of a stock solution containing UV/vis-active guest and CB[6] or CB[7] to a cell containing the UV/vis-active guest in 50 mM  $\text{NaO}_2\text{CCD}_3$ -buffered  $\text{D}_2\text{O}$  (pD 4.74) at 25 °C. The tabulated values of absorbance as a function of CB[7] concentration were fitted to a 1:1 binding model using Associate 1.6.<sup>54</sup>

**$^1\text{H}$  NMR Experiments.**  $^1\text{H}$  NMR competition experiments were performed on a 400 MHz NMR spectrometer; and the temperature was maintained at  $298 \pm 0.5$  K with a temperature control module that had been calibrated using the separation of the resonances of methanol.  $T_1$  relaxation times for guests and their host–guest complexes were measured by the standard inversion recovery experiment. Each sample contained CB[6], CB[7], or CB[8] and an excess of the two competitive guests.  $^1\text{H}$  NMR spectra were acquired with a delay time of 5 times the longest  $T_1$  to ensure that systematic errors due to differences in relaxation times were eliminated. We integrated the resonances corresponding to bound and free guest in uncluttered regions of the spectrum (e.g. 0 to –1 ppm for **12** or **19** and 7.5–6.0 ppm for **11**), which allowed determination of the concentration of the free guests and the two host–guest complexes. Equations 1–3 define the thermodynamics of the host–guest and competition experiments. Substitution of the various concentrations measured by NMR into eq 4 yielded a value of  $K_{rel}$ . The  $K_{rel}$  values were then referenced to the absolute  $K_a$  determined by UV/vis titration using eq 5.



$$K_{rel} = ([\text{CB}[n]\cdot\text{G2}][\text{G1}])/([\text{CB}[n]\cdot\text{G1}][\text{G2}]) \quad (4)$$

$$K_{G2} = (K_{G1})(K_{rel}) \quad (5)$$

**Error Analysis.** Error bars associated with the UV/vis titration refer to the standard error of the least-squares fit of the data to a 1:1 binding model. Because our  $K_a$  measurements involve one or more levels of NMR competition, it is critical to provide an estimate of the level of uncertainty associated with each value of  $K_a$ . All of our measurements were performed in triplicate with independently prepared stock solutions at different ratios of the two competing guests. In these triplicate measurements, one set of concentrations resulted in a 50:50 ratio of the two host–guest complexes; in the other two measurements, we perturbed the system in opposite directions (usually  $\approx$  60:40). These triplicate measurements show excellent agreement (usually  $\pm 5\%$  and

(52) Jeon, W. S.; Kim, H.-J.; Lee, C.; Kim, K. *Chem. Commun.* **2002**, 1828–1829.

(53) McCurdy, A.; Jimenez, L.; Stauffer, D. A.; Dougherty, D. A. *J. Am. Chem. Soc.* **1992**, *114*, 10314–10321.

(54) Peterson, B. R. Ph.D. Thesis, University of California, Los Angeles, 1994.

always less than  $\pm 10\%$ ). As a complementary method to assess the error with  $^1\text{H}$  NMR competition experiments, we first determined the standard error associated with the  $^1\text{H}$  NMR based measurement of a known concentration of guest and host-guest complex ( $\pm 3\%$ ). We then propagated this uncertainty within eq 4 using standard techniques<sup>55</sup> to estimate the error associated with the  $K_{\text{rel}}$  measurement based on a single level of competition ( $\pm 6\%$ ). We use the more conservative estimate of  $\pm 10\%$  for a single  $K_{\text{rel}}$  determination in our error analysis. The errors associated with  $K_{\text{a}}$  values based on one or more levels of competition were then propagated through eq 5 and are reported in Table 1. A sample calculation of the uncertainty associated with the CB[7]·**24** binding constant is given in the Supporting Information.

(55) Bevington, P. R. *Data Reduction and Error Analysis for the Physical Sciences*; McGraw-Hill: New York, 1969.

**Acknowledgment.** We thank the NIH (GM61854) and the University of Maryland for support of this work, Prof. Angel Kaifer for providing compound **14**, and Dr. Anthony Day for a sample of CB[8]. We also thank the reviewers for their insightful comments. L.I. is a Cottrell Scholar of Research Corporation.

**Supporting Information Available:** MMFF-minimized structure of CB[7]·**11**,  $^1\text{H}$  and  $^{13}\text{C}$  NMR spectra for new compounds **3** and **11**, details of the X-ray structures of CB[8]·**3** and CB[8]·**11**, and selected  $^1\text{H}$  NMR spectra from the  $K_{\text{a}}$  and  $K_{\text{rel}}$  determinations. This material is available free of charge via the Internet at <http://pubs.acs.org>.

JA055013X